Available online at www.sciencedirect.com

SciVerse ScienceDirect

Geochimica et Cosmochimica Acta 84 (2012) 614–627

Geochimica et Cosmochimica Acta

www.elsevier.com/locate/gca

An initial investigation into the organic matter biogeochemistry of the Congo River

Robert G.M. Spencer [a,b,*], Peter J. Hernes [c], Anthony K. Aufdenkampe [d], Andy Baker [e], Pauline Gulliver [f], Aron Stubbins [g], George R. Aiken [h], Rachael Y. Dyda [b,c], Kenna D. Butler [h], Vincent L. Mwamba [i], Arthur M. Mangangu [i], Jose N. Wabakanghanzi [i], Johan Six [b]

[a] *Woods Hole Research Center, 149 Woods Hole Road, Falmouth, MA 02540, USA*
[b] *Department of Plant Sciences, University of California, Davis, One Shields Ave, CA 95616, USA*
[c] *Department of Land, Air and Water Resources, University of California, Davis, One Shields Ave, CA 95616, USA*
[d] *Stroud Water Research Center, 970 Spencer Road, Avondale, PA 19311, USA*
[e] *Connected Waters Initiative, Water Research Laboratory, University of New South Wales, 110 King Street, Manly Vale, NSW 2093, Australia*
[f] *NERC Radiocarbon Facility (Environment), SUERC, Rankine Avenue, Scottish Enterprise Technology Park, East Kilbride G75 0QF, UK*
[g] *Skidaway Institute of Oceanography, 10 Ocean Science Circle, Savannah, GA 31411, USA*
[h] *United States Geological Survey, 3215 Marine Street, Boulder, CO 80303, USA*
[i] *Department of Soil Physics and Hydrology, Congo Atomic Energy Commission, P.O. Box 868, Kinshasa XI, People's Republic of Congo*

Received 18 May 2011; accepted in revised form 6 January 2012; available online 11 February 2012

Abstract

The Congo River, which drains pristine tropical forest and savannah and is the second largest exporter of terrestrial carbon to the ocean, was sampled in early 2008 to investigate organic matter (OM) dynamics in this historically understudied river basin. We examined the elemental (%OC, %N, C:N), isotopic ($\delta^{13}C$, $\Delta^{14}C$, $\delta^{15}N$) and biochemical composition (lignin phenols) of coarse particulate (>63 μm; CPOM) and fine particulate (0.7–63 μm; FPOM) OM and DOC, $\delta^{13}C$, $\Delta^{14}C$ and lignin phenol composition with respect to dissolved OM (<0.7 μm; DOM) from five sites in the Congo River Basin. At all sample locations the organic carbon load was dominated by the dissolved phase (~82–89% of total organic carbon) and the total suspended sediment load was principally fine particulate material (~81–91% fine suspended sediment). Distinct compositional and isotopic differences were observed between all fractions. Congo CPOM, FPOM and DOM all originated from vegetation and soil inputs as evidenced by elemental, isotopic and lignin phenol data, however FPOM was derived from much older carbon pools (mean $\Delta^{14}C = -62.2 \pm -13.2‰$, $n = 5$) compared to CPOM and DOM (mean $\Delta^{14}C = 55.7 \pm 30.6‰$, $n = 4$ and $73.4 \pm 16.1‰$, $n = 5$ respectively). The modern radiocarbon ages for DOM belie a degraded lignin compositional signature (i.e. elevated acid:aldehyde ratios (Ad:Al) relative to CPOM and FPOM), and indicate that the application of OM degradation patterns derived from particulate phase studies to dissolved samples needs to be reassessed: these elevated ratios are likely attributable to fractionation processes during solubilization of plant material. The relatively low DOM carbon-normalized lignin yields (Λ_8; 0.67–1.12 (mg(100 mg OC)$^{-1}$)) could also reflect fractionation processes, however, they have also been interpreted as an indication of significant microbial or algal sources of DOM. CPOM appears to be well preserved higher vascular plant material as evidenced by its modern radiocarbon age, elevated C:N (17.2–27.1) and Λ_8 values (4.56–7.59 (mg(100 mg OC)$^{-1}$)). In relation to CPOM, the aged FPOM fraction (320–580 ybp ^{14}C ages) was comparatively degraded, as demonstrated by its nitrogen enrichment (C:N 11.4–14.3), lower Λ_8 (2.80–4.31 (mg(100 mg OC)$^{-1}$)) and elevated lignin Ad:Al values similar to soil derived OM. In this study we observed little modification of the OM signature from sample sites near the cities of Brazzaville and Kinshasa to the head of the estuary (~350 km) highlighting the potential for future studies to assess

* Corresponding author. Tel.: +1 508 444 1572.
E-mail address: rspencer@whrc.org (R.G.M. Spencer).

0016-7037/$ - see front matter
doi:10.1016/j.gca.2012.01.013

seasonal and long-term OM dynamics from this logistically feasible location and derive relevant information with respect to OM exported to the Atlantic Ocean. The relative lack of OM data for the Congo River Basin highlights the importance of studies such as this for establishing baselines upon which to gauge future change.

1. INTRODUCTION

Fluvial systems act as conduits between the biogeochemical cycles of terrestrial and marine ecosystems. In addition rivers are increasingly recognized as significant biogeochemical processors of terrestrially derived organic matter (OM) within the global carbon cycle (Mayorga et al., 2005; Cole et al., 2007; Battin et al., 2008,2009; Aufdenkampe et al., 2011). Due to the multiple sources of OM to rivers, and the different controls with respect to carbon processing and exchange (e.g. tropical to Arctic environments, seasonally inundated areas, organo-mineral complexation, etc.) the reactivity and chemistry of various fractions of dissolved and particulate OM (DOM and POM) vary between and within fluvial systems (Mayorga et al., 2005; Aufdenkampe et al., 2007; Bouillon et al., 2009). One system where these sources and controls have been studied in depth is the Amazon River Basin, where detailed geochemical analyses were conducted on three distinct fractions of riverine OM; coarse particulate OM (CPOM, >63 μm), fine particulate OM (FPOM, 0.7–63 μm) and dissolved OM (DOM, <0.7 μm). These studies demonstrate that Amazon CPOM, FPOM and DOM are compositionally distinct and thus play different roles within the Amazon River Basin (Hedges et al., 1986,1994,2000). Further studies have delivered a comprehensive assessment of carbon biogeochemical processing in the Amazon River Basin (Richey et al., 2002; Mayorga et al., 2005).

Unfortunately, the number of studies focused on the Amazon is a striking exception with only a few other major river-systems examined in terms of carbon processing, for example the Ganges–Brahmaputra (Galy et al., 2007,2008), the Fly-Strickland system (Alin et al., 2008) and the Yukon River Basin (Striegl et al., 2007; Spencer et al., 2008). Tropical river-systems have disproportionally high carbon transport and outgassing compared to temperate and Arctic rivers, yet are underrepresented in global estimates (Aitkenhead and McDowell, 2000; Battin et al., 2008; Aufdenkampe et al., 2011). In addition, many tropical river-systems are facing a range of local pressures including land-use change and associated impacts (e.g. deforestation, conversion to agriculture, increases in discharge, incidence of fire) and global pressures (e.g. increasing temperatures, shifts in precipitation patterns and intensity), all of which impact the mobilization, transport, processing and deposition of carbon and minerals to and within river basins (e.g. Soares-Filho et al., 2006; Laporte et al., 2007; Coe et al., 2009,2011; Aragao and Shimabukuro, 2010). With these points in mind this study provides the first detailed investigation of OM and carbon processing in the Congo River Basin.

The Congo is the largest river in Africa and the second largest river in the World after the Amazon in terms of drainage basin size ($\sim 3.7 \times 10^6$ km^2) and water discharge (Runge, 2007; Laraque et al., 2009). In contrast to the well studied Amazon, the Congo has a very low total suspended sediment (TSS) yield (8.5 Mg km^{-2} yr^{-1}) and despite its discharge is only ranked twelfth in the World with respect to annual TSS load. However, Congo TSS has been reported to have high particulate organic carbon (POC) content and therefore ranks fifth in terms of annual POC flux to the oceans at 2 Tg yr^{-1} (Mariotti et al., 1991; Coynel et al., 2005). With respect to dissolved organic carbon (DOC) the Congo is estimated to export 12.4 Tg yr^{-1}, which for comparison is equivalent to the DOC loads of the three largest Arctic Rivers (Yenisey, Lena and Ob) combined, or greater than six times that of the Mississippi (Coynel et al., 2005; Raymond et al., 2007). Combining DOC and POC loads, the Congo exports 14.4 Tg yr^{-1}of organic carbon to the Atlantic Ocean and is the second major exporter of terrestrial carbon to the oceans after the Amazon (Coynel et al., 2005). The Congo also drains the second largest area of tropical rainforest in the World (~18% of the total global tropical rainforest) and much of the rainforest within the Congo Basin is still in a pristine state, especially within the borders of the Democratic Republic of Congo (DR Congo), with currently just 1% forest disturbance estimated (Laporte et al., 2007).

Despite the apparent importance of the Congo Basin in terms of global carbon budgets the ability to conduct research in the region has been affected by political instability, civil unrest, war and limited infrastructure (Baccini et al., 2008; Prunier, 2008). However, as peace and stability return to the region enabling trade and investment, industrial logging, conversion of pristine forest to agricultural lands and settlement expansion are growing threats to the Congo Basin's forest (Laporte et al., 2007; Koenig, 2008). Therefore, a primary goal of this study was to improve the understanding of carbon dynamics within the Congo River Basin and to determine a baseline against which future studies can gauge impacts. Previous studies on the Congo River-estuary system have estimated TSS, POC and DOC fluxes (Coynel et al., 2005; Laraque et al., 2009) and examined estuarine dynamics (Eisma and Van Bennekom, 1978; Cadee, 1984; Pak et al., 1984). However, to date only limited biochemical composition or isotope data exists for Congo River OM (Mariotti et al., 1991; Spencer et al., 2009,2010a; Stubbins et al., 2010). Firstly, this study provides an initial assessment of the sources of OM within the Congo River via elemental (%OC, %N, C:N), isotopic (δ^{13}C, Δ^{14}C, δ^{15}N), and biochemical compositional (lignin phenols) data for CPOM, FPOM and DOM with a focus on the last ~350 km of the river to the head of its estuary. As well as four sites on the river mainstem an additional sample site was examined (small savannah stream). Although we recognize the limitations of a single

sample site, this site was chosen to assess OM composition in a small order tributary with strong connectivity between terrestrial and aquatic environments, and thus little time for degradative processes in-river in comparison to the mainstem sites. Secondly, we examine the impact of the Malebo Pool (a major widening of the river) and downstream rapids on the quantity and composition of OM exported to the Atlantic. Understanding the influence of river morphology on OM in this region is especially important, as existing budgets have been determined upstream of the rapids. Logistical constraints mean that future studies will likely also focus above the rapids with respect to time series sampling to assess seasonal OM dynamics as well as to set baselines for examination of ongoing perturbation within the Basin. Thus we evaluate whether sampling at Brazzaville–Kinshasa provides relevant information with respect to OM exported to the Atlantic Ocean.

2. MATERIALS AND METHODS

2.1. Study site

The Congo River rises from headwaters located in the south-eastern part of the DR Congo, near the border with Zambia (Runge, 2007). From its headwaters it flows in a generally northern direction, receiving numerous tributaries that enter predominantly from the east, and drain the western slopes of the Central African Rift Valley. Near Kisangani at the Wagenia Falls (Boyoma Falls, formerly Stanley Falls) the river officially becomes known as the Congo. As the Congo flows on toward Mbandaka it turns southwestward and passes through the world's largest swamp forest in the central depression (Cuvette Congolaise or Cuvette Centrale) and the major tributaries of the Ubangui (Oubangui), Sangha and the Kasai join prior to the Congo entering the Pool Malebo (Fig. 1). At this major widening of the Congo River, the cities of Kinshasa (population ~10 million, capital of DR Congo) and Brazzaville (population ~1.5 million, capital of Republic of Congo) lie across the Malebo Pool from one another. The Congo River then drops ~270 m through a series of falls and rapids (Livingstone Falls) over 350 km and narrows considerably down to the port of Matadi (Fig. 1). Downstream, the Congo widens again (up to 19 km) with abundant large sand bars and at Boma (~100 km from the mouth) the Congo becomes tidally influenced (Runge, 2007).

The Congo River discharge near its mouth at Kinshasa exhibits an exceptionally stable intra-annual regime (MaxQ/MinQ = 1.94, 1977–2006 inclusive) as its basin straddles the Equator and thus receives rainfall in at least one part of its basin throughout the year. The Congo at Kinshasa has a bimodal hydrological cycle with maximum flows in December and May and minimum flows in August and March (Fig. 2). The greater discharge maximum in December relates to the period of increased discharge from the northern tributaries (e.g. the Ubangui) and is complemented by the southern tributaries whose water discharges start to increase at about the same time. This period represents the time of maximum carbon (especially DOC) export as the Cuvette Congolaise is brought into the hydrologic flow path of the river (Coynel et al., 2005). The smaller discharge maximum in May is due to an increase from the southern part of the basin and is dominated by DOC from rivers draining areas of savannah vegetation (Coynel et al., 2005). The Congo at Kinshasa also has a very stable discharge regime from year to year with an interannual ratio of 1.62 from 1977–2006 inclusive. The monthly mean discharge at Kinshasa from 1977–2006 ranged from 30,060–54,538 $m^3 s^{-1}$ (monthly median = 29,648–53,196 $m^3 s^{-1}$; maximum = 35,488–63,516 $m^3 s^{-1}$; minimum = 24,420–43,101 $m^3 s^{-1}$; Fig. 2).

2.2. Sampling locations

Samples were collected in January and February 2008 from five locations in the Congo River Basin (Fig. 1; Table 1) and predominantly focused on the lower mainstem of the Congo River toward the estuary (Fig. 1a and c). Sites 1 and 2 were upstream and downstream of the Malebo Pool respectively. Sites 3 and 4 were further downstream, with site 3 below the lower Congo rapids, and site 4 toward the head of the estuary (Fig. 1a and c; Table 1). Therefore, sites 3 and 4 allow a comparison to site 2 to examine the influence of the lower Congo rapids and subsequent widening of the river down from Boma on TSS and OM dynamics prior to export to the Atlantic Ocean. This is particularly important as existing budgets for TSS, POC and DOC for export via the Congo River have been derived primarily from sampling near Brazzaville (e.g. Coynel et al., 2005; Laraque et al., 2009). Finally, site 5 was on the Luilu River in the Kasai-Oriental Province in southern DR Congo, a tributary of the Sankuru River, which drains into the Kasai River, the major southern tributary of the Congo (Fig. 1a and b; Table 1). This site is typical of the numerous small tributaries that drain vast areas of savannah and grassland throughout the Congo Basin.

2.3. Ancillary measurements, sample collection and processing

Temperature, pH, conductivity and salinity were measured *in situ* using a portable multiparameter probe (Horiba model U-10) and pH was cross-checked with a combination pH electrode (Mettler Toledo). Water samples were collected from boats at sites 1–4 and from a bridge at site 5 via a submersible pump from 6/10 of the total river depth in the thalweg where suspended sediment size distributions are most representative of depth-integrated fluxes (Aufdenkampe et al., 2007). The depth of the river was monitored via a digital sonar fish finder (Hummingbird 100SX) mounted on a wooden float board. At all sites ~40 L of water was collected.

Coarse suspended sediment (CSS) concentrations were quantified from a sample collected by passing a known volume of pumped water through a sieve with a 63 μm Nitex screen. Larger amounts of CSS and CPOM for geochemical and isotopic analyses were collected at each site with a plankton net constructed from a 63 μm Nitex screen. Seived water was then placed into a churn sample splitter (Bel-Art) and the sample was carefully homogenized while

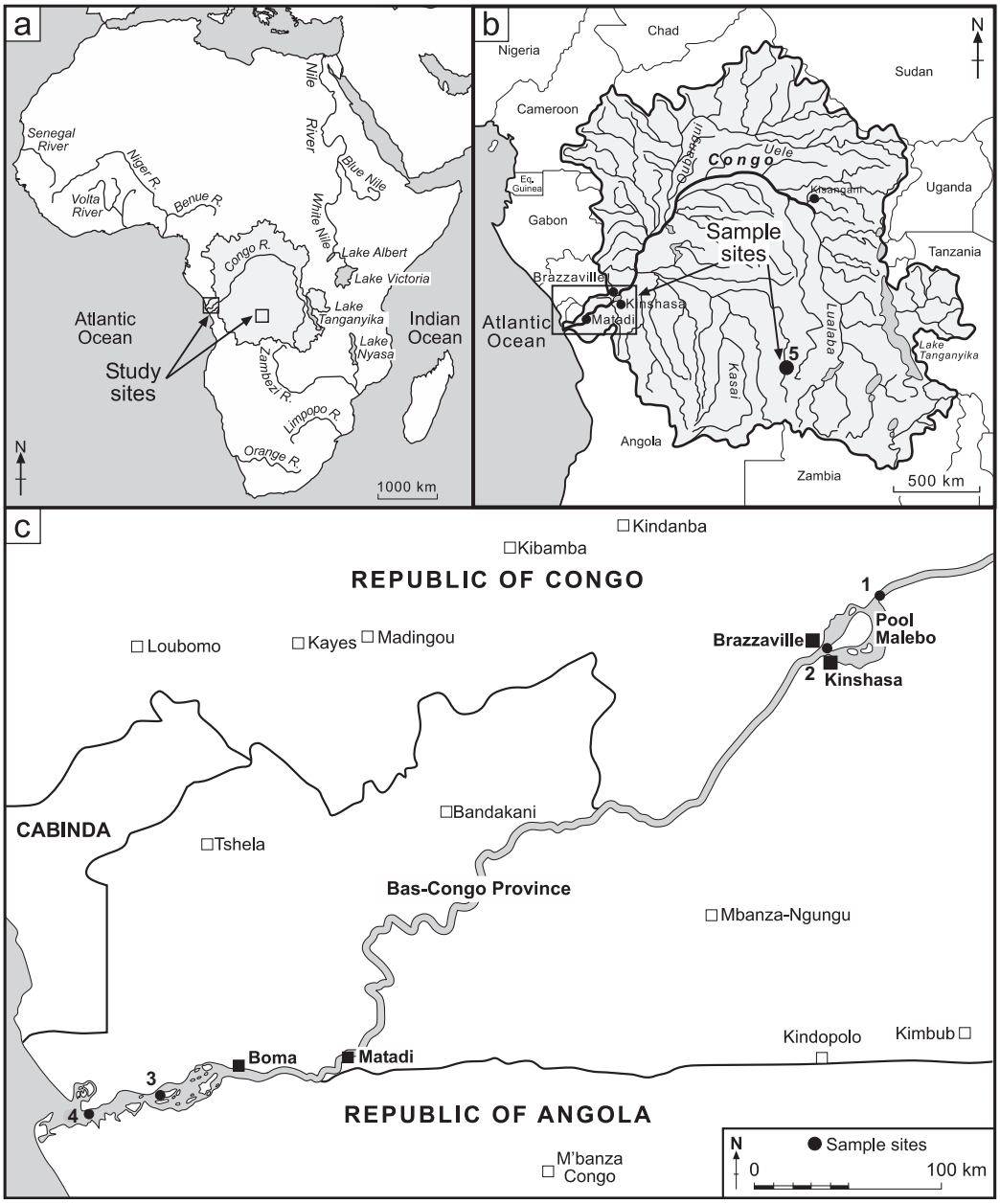

Fig. 1. (a) Map of the Congo River Basin within Africa showing the study sites. (b) The sample sites within the Congo Basin highlighting the location of site 5 (numbered black circle) and the inset box covers the region shown in detail in Fig. 1c. (c) Sample sites 1–4 (numbered black circles).

subsampling for fine suspended sediments (FSS) and FPOM. FSS concentrations were determined gravimetrically by filtration of 250–500 mL of water onto preweighed membrane filters (Millipore HAWP, 0.45 μm). FPOM samples were collected by filtering 250–500 mL of water through preweighed and precombusted (with respect to glass and quartz filters; 550 °C) membrane filters (Millipore HAWP, 0.45 μm), glass fiber filters (Whatman GF/F, 0.7 μm) and quartz filters (Pall, 0.7 μm). All CSS, CPOM, FSS and FPOM samples were dried at the end of each sample day and stored frozen until analysis. Samples for DOM analyses were filtered through precombusted (550 °C) glass fiber filters (Whatman GF/F, 0.7 μm) and then the filtrate was stored frozen (−20 °C).

2.4. Organic matter analyses

CPOM and FPOM were wetted with Milli-Q and fumed with HCl (Baker Analyzed) vapors for 18 h, effectively removing carbonates for isotopic analyses while avoiding potential nitrogen contamination from ammonium in the acid. Subsamples were analyzed on an elemental analyzer (EA; Costech ECS 4010) interfaced with an isotope ratio mass spectrometer (IRMS; Thermo-Finnigan DeltaPlus

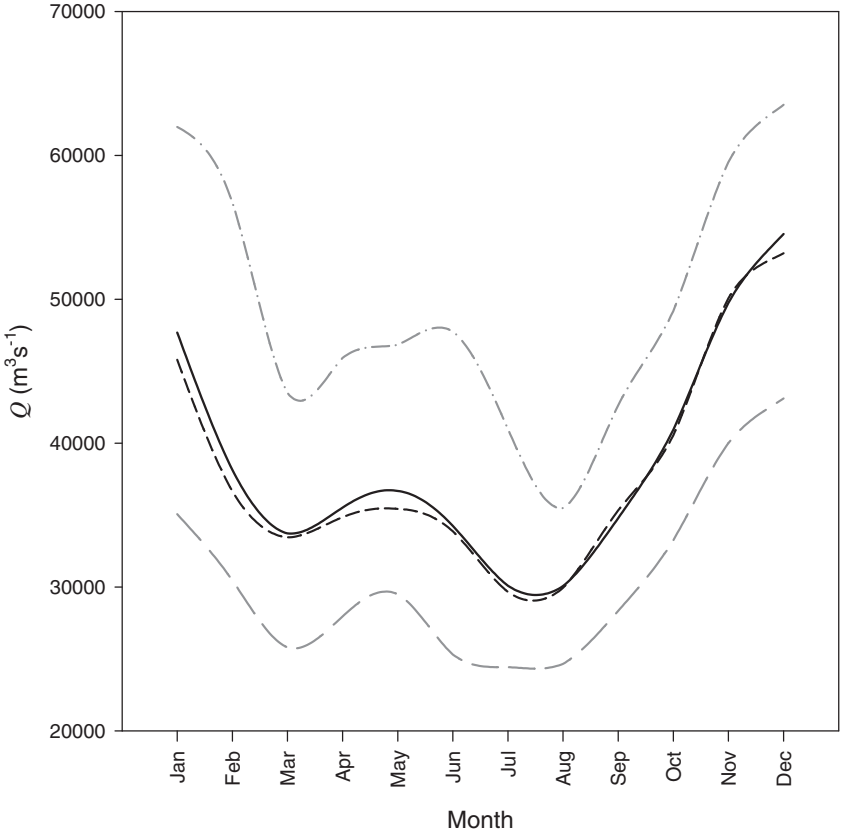

Fig. 2. Discharge data from the Congo River at Kinshasa station (30 year average, 1977–2006); mean (solid black line); median (dashed black line); maximum (dash-dot gray line) and minimum (long dash gray line).

Table 1
Sample locations and physicochemical characteristics.

Site #	Location	Lat. (°S)	Lon. (°E)	Temp. (°C)	pH	Salinity
1	Maluku	04.0502	15.3136	28.7	6.45	<0.1
2	Kinshasa	04.1815	15.2058	28.8	6.46	<0.1
3	Ile de Mateba	05.5735	12.4913	28.6	6.46	<0.1
4	Kimuabi	06.0313	12.3116	28.5	6.54	0.2
5	Luilu	07.0356	23.3545	27.9	6.64	<0.1

XP). Standard curves were created using four isotopically enriched and 4–5 isotopically depleted L-glutamic acid standards prepared over a range that encompassed the carbon and nitrogen amounts in the samples. These laboratory standards were referenced to USGS-41 ($\delta^{13}C = +37.63‰$, $\delta^{15}N = +47.57‰$) and USGS-40 ($\delta^{13}C = -26.39‰$, $\delta^{15}N = -4.52‰$) and normalized relative to the Vienna Pee Dee Belemnite and Air (Coplen et al., 2006). FPOM was quantitatively subsampled from the glass fiber filter by punching a known area of filter and sediment, which are not easily separated from one another. FPOC concentration (mg L^{-1}) was calculated from the mass of the carbon analyzed (quantified by EA), the fraction of total filter analyzed (fraction of filtered area that was punched out) and the volume of water filtered. Weight percent organic carbon (%OC) and nitrogen (%N) of FPOM was calculated as the ratio of FPOC or FPN (mg L^{-1}) to FSS (mg L^{-1}). The average relative uncertainties for %OC, %N and molar C:N were ±0.8%, ±2.5% and ±0.3% for FPOM and ±1.6%, ±4.5% and ±1.0% for CPOM, respectively. DOC was analyzed via high temperature combustion with non-dispersive infrared detection (Shimadzu TOC 5000) using previously described methods (Spencer et al., 2009). All DOC data are the mean of three to five replicate injections for which the coefficient of variance was less than 2%.

For particulate samples $\delta^{13}C$ and $\delta^{15}N$ were determined by a Thermo-Finnigan DeltaPlus XP isotope ratio mass spectrometer (IRMS) (precision of ±0.1‰ for $\delta^{13}C$ of CPOM and ±0.3‰ for $\delta^{13}C$ of FPOM and $\delta^{15}N$ of CPOM and FPOM) and $\delta^{13}C$–DOC samples were analyzed using an O.I. Analytical Model 1010 TOC analyzer (precision of ±0.2‰) interfaced to a PDZ Europa 20–20 IRMS (Sercon Ltd.) (Aufdenkampe et al., 2007; Spencer et al., 2009).

δ^{13}C-DOC measurements were calibrated against the δ^{13}C values of KHP and IHSS Suwannee River humic acid in Milli-Q, and blank corrections were conducted following the procedures of Osburn and St-Jean (2007).

Radiocarbon analyses were undertaken at the Natural Environment Research Council Radiocarbon Facility (U.K.) where they were pretreated according to sample type. DOC samples were acidified to pH 2 using 1 M HCl followed by purging with high purity N_2 for 10 min to remove inorganic carbon. Samples were then neutralized to pH 7 using 1 M KOH before rotary evaporation (40 °C; 50 mbar), until a few mL of solution remained. This concentrate was then transferred to precombusted glass beakers, lyophilized and the resultant solid homogenized. Milli-Q blanks were analyzed to check for any potential contamination issues in DOC processing and none were observed. CPOC samples were acid washed overnight in 1 M HCl at 20 °C to remove inorganic carbon, dried and homogenized. DOC solids and CPOC were converted to CO_2 by sealed tube combustion where a known weight of the pretreated material was heated with CuO in an evacuated sealed quartz tube (Boutton et al., 1983). FPOC samples were separated as much as possible from their associated quartz filter and then converted to CO_2 by combustion using a Costech ECS 4010 elemental combustion system. Irrespective of the means of combustion, sample CO_2 was cryogenically purified and the volume recorded before the gas was collected in aliquots. One aliquot was converted to graphite by Fe/Zn reduction and the resultant graphite analyzed for Δ^{14}C content at the Scottish Universities Environmental Research Center (U.K.) accelerator mass spectrometer (AMS) laboratory using a 250 kV single-stage AMS (SSAMS). In keeping with international practice Δ^{14}C results have been corrected to a $\delta^{13}C_{V\text{-}PDB}$ value of −25‰ using the δ^{13}C of each sample and are presented using the Δ notation (‰) with a $\pm 1\sigma$ level for overall analytical confidence (Stuiver and Polach, 1977; van der Plicht and Hogg, 2006).

Lignin phenols were measured using the alkaline CuO oxidation method of Hedges and Ertel (1982) with modifications as outlined in detail by Spencer et al. (2010b). In brief, whole water samples (250 mL) for sites 1–5 were acidified to pH 2 with 12 N HCl and then rotary evaporated to ~3 mL. FPOM samples on Millipore HAWP, 0.45 μm membrane filters were sonicated in small volumes of Milli-Q water which removed the FSS into suspension and the membrane filters were subsequently removed. The concentrates, elutes or suspensions were transferred to Monel reaction vessels (Prime Focus, Inc.) and dried under vacuum centrifugation. Dried CPOM samples (~100 mg) were directly placed into Monel reaction vessels. Samples were then oxidized in a stoichiometric excess of CuO, followed by acidification and ethyl acetate extraction. Following redissolution in pyridine, lignin phenols were silylated with *N*/*O* bis-trimethylsilyltrifluoromethylacetamide (BSTFA) and quantification was carried out on a gas chromatography – mass spectrometer (Agilent 6890 gas chromatograph equipped with an Agilent 5973 mass selective detector and a DB5-MS capillary column; 30 m, 0.25 mm inner diameter, Agilent) using cinnamic acid as an internal standard and a five point calibration scheme (Spencer et al., 2010b). Eight lignin phenols (three vanillyl phenols, three syringyl phenols and two cinnamyl phenols) were quantified for all samples. All samples were blank corrected and at least one blank was run for every ten samples. Blank concentrations of lignin phenols were low (30–40 ng) and therefore never exceeded 2% of the total lignin phenols in a sample.

3. RESULTS

3.1. Physicochemical characteristics, OM concentrations and elemental compositions

Water temperature and pH showed little variation between mainstem sites 1–4 (28.5–28.8 °C and 6.45–6.54 respectively) and site 5 (small savannah tributary) was slightly cooler and had higher pH (27.9 °C and 6.64 respectively; Table 1). Congo River mainstem (sites 1–4; Table 2) samples ranged in TSS concentration from 18.0–20.3 mg L^{-1}. The lowest TSS concentration (13.2 mg L^{-1}) was found in the Luilu River (site 5; small savannah tributary) (Table 2). Fine suspended sediments (FSS) dominated the TSS load at all sites comprising ~81–85% of the sediment load at sites 1–4, and ~91% at site 5 (Table 2). FPOC and CPOC show a small range through sites 1–4 (1.13–1.44 mg L^{-1} and 0.16–0.34 mg L^{-1} respectively; Table 2). This range of FPOC is comparable to the concentration at site 5 (1.23 mg L^{-1}), however, higher than CPOC at that site (0.08 mg L^{-1}). The distribution of organic carbon between CPOC, FPOC and DOC size fractions (Table 2; Fig. 3) shows the dominance of DOC at all sites. The percent DOC of TOC ranged from 82.3% to 89.2% and was lowest at site 5 in the small savannah tributary. Mainstem sites 1–4 show a narrow range in the DOC concentration (10.5–10.7 mg L^{-1}) and in the percent of TOC derived from DOC ranging from 85.7 to 89.2% (Table 2; Fig. 3).

Table 2
Sediment and organic carbon concentrations; not determined (——).

Site #	TSS (mg L^{-1})	CSS (mg L^{-1})	FSS (mg L^{-1})	CPOC (mg L^{-1})	FPOC (mg L^{-1})	DOC (mg L^{-1})	TOC (mg L^{-1})	DOC/TOC (%)
1	18.0	2.8	15.2	0.16	1.13	10.7	12.0	89.2
2	20.3	3.9	16.4	0.24	1.15	10.7	12.1	88.5
3	18.9	3.3	15.6	——	1.37	10.5	——	——
4	19.7	2.9	16.8	0.34	1.44	10.7	12.5	85.7
5	13.2	1.2	12.0	0.08	1.23	6.1	7.4	82.3

CPOM had higher molar organic carbon to nitrogen ratios (C:N; 17.2–27.1) than the FPOM (11.4–14.3) (Table 3). Mainstem sites 1–4 had a narrow range of C:N for CPOM and FPOM between 17.2–20.4 and 11.4–12.5 respectively. Site 5, the small savannah tributary, had the highest FPOM C:N (14.3) and also the highest CPOM C:N (27.1).

3.2. Stable and radiocarbon isotopes

Stable carbon isotopic values ranged from −26.6‰ to −29.2‰ across the CPOC, FPOC and DOC size fractions (Table 3). For mainstem sites 1–4 an enrichment in $\delta^{13}C$ is observed in CPOC (mean = −26.9 ± −0.3‰, $n = 3$) relative to FPOC (mean = −28.2 ± −0.5‰, $n = 4$), which in turn is enriched relative to DOC (mean = −29.2 ± −0.1‰, $n = 4$). Site 5 shows no difference between FPOC and DOC (−27.9 ‰), but a slight relative depletion in the CPOC (−28.7 ‰; Table 3). In conjunction with the depletion in the $\delta^{13}C$ signature between CPOM and FPOM for mainstem sites 1–4 the $\delta^{15}N$ isotopic values typically show an enrichment from 4.7 ± 0.4‰, ($n = 3$) to 5.5 ± 0.5‰, ($n = 4$). A similar enrichment in $\delta^{15}N$ was observed at site 5 between CPOM and FPOM from 2.1‰ to 3.0‰ (Table 3).

Radiocarbon ($\Delta^{14}C$) values across the three OC fractions ranged from 95.7‰ to −69.7‰ (>modern to 580 ybp; Table 3). The $\Delta^{14}C$-CPOC samples ranged from 23.9‰ to 60.6‰ (mean = 42.4 ± 18.4‰, $n = 3$) for mainstem sites 1–4 and showed slight enrichment in the small savannah tributary (site 5; 95.7‰). The $\Delta^{14}C$-DOC pool was also enriched in bomb carbon in comparison to modern atmospheric values and ranged from 50.4‰ to 93.7‰ across the study sites (mean = 73.4 ± 16.1‰, $n = 5$). The $\Delta^{14}C$-FPOC values, however, were depleted in comparison to both the CPOC and DOC fractions with mainstem sites 1–4 ranging from −39.0‰ to −69.7‰ (mean = -−61.7 ± −15.2‰, $n = 4$) which is comparable to the value for $\Delta^{14}C$-FPOC observed at site 5 (small savannah tributary; −63.9 ‰) and so appears to be typical of the age of FPOC in the Congo Basin (Table 3).

3.3. Lignin phenols

Carbon-normalized lignin yields in this manuscript refer to the sum of three vanillyl phenols (V), plus three syringyl phenols (Λ_6), plus the two cinnamyl phenols (Λ_8), respectively. Total yields for V, Λ_6 and Λ_8 were greatest for CPOM samples, then FPOM samples and lowest in DOM samples (Table 4). CPOM V, Λ_6 and Λ_8 values showed little variation between mainstem sites 1–4 ranging from 2.05 to 2.34 (mean = 2.23 ± 0.16; $n = 3$), 3.93 to 4.10 (mean = 4.02 ± 0.09; $n = 3$) and 4.56 to 5.01 (mean = 4.78 ± 0.23; $n = 3$) (mg(100 mg OC)$^{-1}$) respectively. In comparison CPOM V, Λ_6 and Λ_8 values for site 5 were elevated at 3.28, 6.38 and 7.59 (mg(100 mg OC)$^{-1}$) respectively. FPOM and DOM V, Λ_6 and Λ_8 values also showed little variation between mainstem sites 1 and 4 (Table 4). For example, FPOM and DOM Λ_8 samples 1–4 ranged from 2.80 to 2.97 (mean = 2.88 ± 0.07; $n = 4$) and 0.67–0.72 (mean = 0.69 ± 0.02; $n = 4$) (mg(100 mg OC)$^{-1}$) respectively with no apparent downstream trend. As reported for CPOM, in comparison to sites 1–4, V, Λ_6 and Λ_8 values at site 5 for FPOM were elevated at 2.21, 4.07 and 4.31 (mg(100 mg OC)$^{-1}$) respectively. DOM V, Λ_6 and Λ_8 values were also elevated for site 5 (0.53, 1.00, 1.12 (mg(100 mg OC)$^{-1}$)) in comparison to sites 1–4.

Cinnamyl:vanillyl (C:V) and syringyl:vanillyl phenol (S:V) ratios in the CPOM, FPOM and DOM fractions were constant in mainstem sites 1–4 and higher ratios were observed in the CPOM fraction (0.22–0.24) versus the FPOM fraction (0.10–0.12; Table 4). CPOM and FPOM C:V and S:V ratios were relatively constant at all sites but CPOM C:V values were higher for site 5 (0.37), the small savannah tributary. Sites 5 also had higher C:V and S:V ratios in DOM than the mainstem sites (Table 4). Vanillic acid to vanillin ($(Ad:Al)_v$) and syringic acid to syringaldehyde ($(Ad:Al)_s$) values showed a clear trend with OM fraction with ratios increasing from CPOM to FPOM to DOM (Table 4). $(Ad:Al)_v$ and $(Ad:Al)_s$ values for the CPOM and FPOM fractions were relatively constant for mainstem sites, but at site 5 the CPOM and FPOM $(Ad:Al)_v$ and $(Ad:Al)_s$ values were slightly lower than for the mainstem sites. Within the DOM pool $(Ad:Al)_v$ and $(Ad:Al)_s$ values were also constant in mainstem sites 1–4 ranging from 1.37 to 1.39 (mean = 1.38 ± 0.01; $n = 4$) and 1.11–1.13 (mean = 1.12 ± 0.01; $n = 4$) respectively, but at site 5 the $(Ad:Al)_s$ value was lower (0.78; Table 4) than on the mainstem.

4. DISCUSSION

4.1. Organic matter distribution

The TSS concentrations measured at the Congo River mainstem sites (1–4; Table 2) are similar to previous studies focused on this region of the river at the same point in the annual hydrograph (~24–26 mg L^{-1}; Mariotti et al., 1991; Coynel et al., 2005). In comparison to other major global rivers the Congo has a relatively low TSS concentration at all sites within the basin (1–5), particularly in relation to other tropical rivers such as the Amazon, Fly and Strickland (Richey et al., 1986; Ludwig and Probst, 1998; Coynel et al., 2005; Alin et al., 2008). Concentrations of CPOC, FPOC and DOC for mainstem sites 1–4 were also highly comparable to previous data from this location and point on the hydrograph (e.g. high water values for POC and DOC ~1.5 and 11.0 mg L^{-1} respectively (Coynel et al., 2005); Fig. 3; Table 2) and demonstrate the organic-rich character of the Congo. Mainstem CPOM and FPOM %OC values (5.7–11.8% and 7.0–8.8% respectively; Table 3) were elevated in comparison to similar samples from the Amazon Basin, where typically CPOM and FPOM %OC range from 0.3–4.7% and 0.4–2.0%, and Amazon mainstem sites at Obidos are typically around 1.0% and 1.21% respectively (Hedges et al., 1986, 2000; Aufdenkampe et al., 2007). Congo CPOM and FPOM %OC values are also high in comparison to data from the Fly and Strickland Rivers in Papua New Guinea (CPOM: Strickland = 1.5%, Fly = 0.9%: FPOM: Strickland = 1.8%, Fly = 5.5%; Alin et al., 2008). Variation in %OC values can be related to

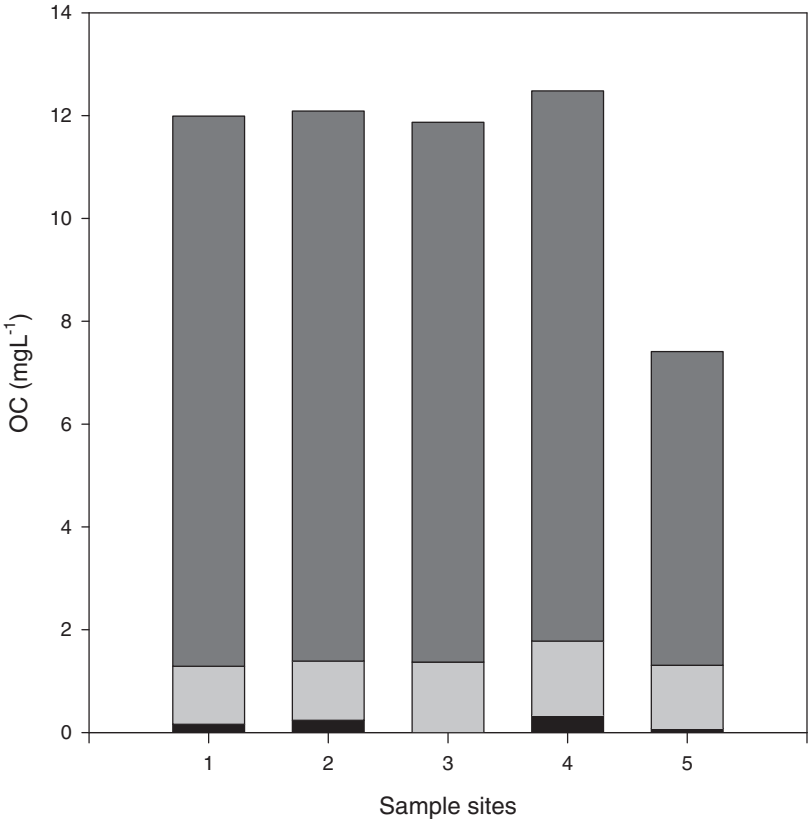

Fig. 3. The concentration of total organic carbon for the samples sites partitioned into the coarse (black shading) and fine (light gray shading) particulate fractions (CPOC and FPOC respectively) and the dissolved (dark gray shading) fraction (DOC). N.B. Site 3 does not include CPOC as this sample was lost.

Table 3
Organic carbon and nitrogen distributions, compositions and radiocarbon data; not determined (——).

Site	Fraction	OC (wt.%)	N (wt.%)	C:N (molar)	$\Delta^{14}C$ (‰)	^{14}C Age (ybp)	$\delta^{13}C$ (‰)	$\delta^{15}N$ (‰)
1	CPOM	5.7	0.4	17.2	60.6	Modern	−26.9	4.9
2	CPOM	6.0	0.4	18.0	42.6	Modern	−27.2	4.9
3	CPOM	——	——	——	——	——	——	——
4	CPOM	11.8	0.7	20.4	23.9	Modern	−26.6	4.3
5	CPOM	6.7	0.3	27.1	95.7	Modern	−28.7	2.1
1	FPOM	7.4	0.7	12.2	−69.7	580	−28.3	4.7
2	FPOM	7.0	0.7	12.5	−69.2	576	−28.8	5.5
3	FPOM	8.8	0.9	11.4	−69.0	575	−27.6	5.9
4	FPOM	8.5	0.8	12.1	−39.0	320	−28.2	5.7
5	FPOM	10.2	0.8	14.3	−63.9	530	−27.9	3.0
1	DOM	——	——	——	78.9	Modern	−29.2	——
2	DOM	——	——	——	93.7	Modern	−29.2	——
3	DOM	——	——	——	77.6	Modern	−29.1	——
4	DOM	——	——	——	66.6	Modern	−29.1	——
5	DOM	——	——	——	50.4	Modern	−27.9	——

mineral surface area (Aufdenkampe et al., 2007). Thus, we propose two possible explanations for the high %OC of FPOM or in reality a combination of these may be occurring. Firstly, the fine suspended minerals could have a very high specific surface area, such as found for iron and aluminum oxides that can leach and then re-precipitate under less acidic and more oxygenated conditions (Kaiser and Guggenberger, 2003 ; Aufdenkampe et al., 2007). This is not

unlikely given the Congo Basin's extensive high iron "ferralitic" soils and also the lack of highly eroding mountainous headwaters that might deliver alumina-silicate clays with lower specific surface area (Sys, 1960). The second explanation might be that the very high DOC/TSS ratio of the Congo causes higher loadings of carbon onto fine minerals, as occurs with adsorption isotherms that have not yet reached saturation (Qualls and Haines, 1992).

Congo CPOM C:N ranged from 17.2 to 27.1, which is highly comparable to previous data from the Amazon mainstem and major lower Amazon tributaries (15.3–29.8; Hedges et al., 1986,1994). This range for C:N is analogous to leaves from a variety of tropical plant species and the low density, mineral free organic debris fraction in soils (Hedges et al., 1986; Hedges and Oades, 1997; McGroddy et al., 2004) indicating Congo CPOM to be minimally degraded either prior to or after entrainment into the hydrologic pathway of the river. Congo FPOM C:N values were lower (11.4–14.3) than CPOM values, and highly comparable to Amazon Basin FPOM C:N values (6.8–13.2; Hedges et al., 1986,1994). This relative enrichment of nitrogen in FPOM may result from nitrogen immobilization in microbial biomass and degradation products, as well as preferential sorption of nitrogen-containing compounds (Post et al., 1985; Aufdenkampe et al., 2001).

4.2. Organic matter isotopic composition

Stable and radiocarbon isotopes have a long history of use for examining OM source and history in rivers and coastal margins (Mariotti et al., 1991; Hedges et al., 1997; Raymond and Bauer, 2001; Mayorga et al., 2005). The $\delta^{13}C$ and $\delta^{15}N$ values observed in the Congo OM fractions are highly comparable to previous data from Amazon Basin Rivers (e.g. $\delta^{13}C$ −24.2‰ to −29.2‰ and $\delta^{15}N$ 1.9‰ to 5.4‰; Hedges et al., 2000; Table 3). $\delta^{13}C$ values within the Congo were typically enriched in CPOM relative to FPOM, while $\delta^{15}N$ was depleted in CPOM relative to FPOM. This trend is intriguing as one potential explanation for relative enrichment in $\delta^{15}N$ is isotopic fractionation during degradation, as further evidenced by the low FPOM C:N values, but interestingly $\delta^{13}C$ does not show an analogous enrichment as might be expected (Nadelhoffer and Fry, 1988). A similar scenario has been shown in the Fly, Strickland and major lower Amazon tributaries and was attributed to freshwater algae that have highly depleted $\delta^{13}C$ signatures (Hedges et al., 1986; Alin et al., 2008).

At all Congo study sites $\Delta^{14}C$-DOC was modern and had a $\delta^{13}C$ signature indicative of contemporary C_3 plants, as observed in a number of other global rivers from the Arctic to the Amazon (Table 3; Raymond and Bauer, 2001; Benner et al., 2004; Mayorga et al., 2005; Ahad et al., 2006). Similar to DOC, $\Delta^{14}C$-CPOC was also modern throughout the Congo study sites as also observed for lowland rivers in the Amazon (Mayorga et al., 2005). These results highlight the tight coupling between recently fixed terrestrial carbon and export to the Atlantic Ocean for these two fractions. However, $\Delta^{14}C$-FPOC was depleted in relation to both CPOC and DOC with mainstem sites 1–4 (mean = −61.7 ± −15.2‰) and the savannah tributary (site 5; −63.9 ‰) showing typical radiocarbon ages for mineral associated OM in tropical soils (Trumbore, 2000).

4.3. Organic matter biochemical composition

Lignin phenols are unambiguous biomarkers for vascular plant derived OM and their carbon-normalized yields (Λ_8) can be used to assess the vascular plant contribution to the OM pool (Hedges and Mann, 1979; Spencer et al., 2010b). CPOM Λ_8 values for the Congo (Table 4) are in the range previously reported for Amazonian Rivers (Hedges et al., 1986; Aufdenkampe et al., 2007). Congo mainstem (sites 1–4) Λ_8 values are comparable to the mainstem of the Amazon at Obidos (5.92 (mg(100 mg OC)$^{-1}$); Hedges et al., 2000), and the Fly (5.24 (mg(100 mg OC)$^{-1}$)) and Strickland Rivers (4.80 (mg(100 mg OC)$^{-1}$);

Table 4
Lignin phenol parameters; carbon-normalized lignin yields (Λ_8, Λ_6, V), cinnamyl:vanillyl phenol ratios (C:V), syringyl:vanillyl phenol ratios (S:V), vanillic acid:vanillin ratios $(Ad:Al)_v$, syringic acid:syringaldehyde ratios $(Ad:Al)_s$; not determined (——).

Site	Fraction	Λ_8 (mg (100 mg OC)$^{-1}$)	Λ_6 (mg (100 mg OC)$^{-1}$)	V (mg (100 mg OC)$^{-1}$)	C:V	S:V	$(Ad:Al)_v$	$(Ad:Al)_s$
1	CPOM	4.56	3.93	2.05	0.22	0.99	0.50	0.52
2	CPOM	5.01	4.10	2.34	0.24	0.95	0.55	0.51
3	CPOM	——	——	——	——	——	——	——
4	CPOM	4.78	4.03	2.29	0.22	0.91	0.50	0.48
5	CPOM	7.59	6.38	3.28	0.37	0.95	0.39	0.41
1	FPOM	2.90	2.72	1.50	0.12	0.81	1.12	0.85
2	FPOM	2.80	2.69	1.60	0.12	0.81	1.11	0.85
3	FPOM	2.97	2.75	1.62	0.10	0.77	1.21	0.82
4	FPOM	2.84	2.67	1.60	0.10	0.78	1.13	0.86
5	FPOM	4.31	4.07	2.21	0.11	0.84	1.01	0.74
1	DOM	0.72	0.66	0.39	0.15	0.68	1.38	1.11
2	DOM	0.69	0.62	0.38	0.16	0.71	1.39	1.13
3	DOM	0.67	0.62	0.36	0.15	0.71	1.38	1.11
4	DOM	0.69	0.61	0.37	0.16	0.69	1.37	1.11
5	DOM	1.12	1.00	0.53	0.23	0.90	1.38	0.78

Alin et al., 2008) in Papua New Guinea. FPOM Congo Λ_8 values (Table 4) are toward the higher end of previously reported data from the Amazon Basin and considerably higher than observed for the Amazon mainstem at Obidos (1.68 (mg(100 mg OC)$^{-1}$); Hedges et al., 2000). DOM Λ_8 values are also high in comparison to other global rivers further underpinning the high vascular plant inputs to the Congo River. For contrast, a broad suite of rivers in the Yukon River Basin from glacier and groundwater dominated through to peatland draining blackwaters had DOM Λ_8 values ranging from 0.05–0.49 (mg(100 mg OC)$^{-1}$ (Spencer et al., 2008).

The C:N of OM is often combined with Λ_8 to examine OM sources (Fig. 4a) and this provides good discrimination between CPOM and FPOM for the Congo samples. CPOM samples have higher Λ_8 and C:N consistent with high vascular plant inputs derived from tropical tree leaves and woody materials (Hedges et al., 1986). In conjunction with δ^{13}C, Λ_8 values are often used to assess OM contributions from different sources (Fig. 4b). Historically, this type of plot is used to highlight C_3 vegetation described by depleted δ^{13}C values and elevated Λ_8 values (Hedges et al., 1997,2000). In the Congo, however, overlap between the δ^{13}C signatures of the three OM pools due to apparent freshwater algae sources with highly depleted δ^{13}C signatures complicates the Λ_8 versus δ^{13}C relationship. Congo Λ_8 values clearly show a trend with highest values in CPOM, lower values in FPOM and lower values still in the DOM (Table 4; Fig. 4b), and such a trend has previously been reported in Amazon OM fractions (Hedges et al., 1986,2000; Aufdenkampe et al., 2007). A decline in Λ_8 through the size fractions has been attributed in previous studies to the degradation of lignin in the source materials and addition of microbial and fungal derived carbon, thus as Λ_8 decreases it implies greater processing of the OM and an increase in immobilized nitrogen (i.e. lower C:N; Table 3; Fig. 4a). Such processing seems to be supported by other data when examining the trend between CPOM and FPOM (e.g. declining C:N, enrichment in δ^{15}N, the greater radiocarbon age of FPOM), but the DOC has a modern age and so does not appear to fit such a proposed degradation model. Historically, riverine DOM has been described as highly degraded and aged due in part to its biochemical signature and its fate in the ocean has been a topic of great interest (Hedges et al., 1997,2000). A number of recent studies have shown though that the apparent degraded biochemical signature of riverine DOM can actually be attributed to the processes of leaching and sorption (Aufdenkampe et al., 2001; Hernes et al., 2007). For example, with respect to $(Ad:Al)_v$ ratios, Hernes et al., (2007), showed an approximate twofold increase from a range of litters to their respective leachates solely due to solubilization, and a further increase in $(Ad:Al)_v$ ratios following sorption to soil minerals. Furthermore, other studies have shown that riverine DOM can be biolabile concurrent with elevated Λ_8 and a modern radiocarbon age (Raymond et al., 2007; Spencer et al., 2008; Holmes et al., 2008). Thus it seems that the application of OM degradation patterns derived from particulate phase studies needs to be carefully assessed as current evidence implies that partitioning accompanied by fractionation during leaching and sorption and desorption processes can drive the trends observed in the dissolved phase that are often interpreted as degradation signatures. There is also the possibility that low DOM carbon-normalized lignin yields in conjunction with the reported modern Δ^{14}C-DOC and highly depleted δ^{13}C-DOC values points to autochthonous sources of DOM, as in other tropical rivers freshwater algae have exhibited highly depleted δ^{13}C signatures (Hedges et al., 1986; Alin et al., 2008).

The syringyl (S) and cinnamyl (C) phenols are solely present in angiosperms and nonwoody tissues, respectively, and therefore their ratios to the vanillyl phenols (V) allow the discrimination of angiosperm and gymnosperm sources

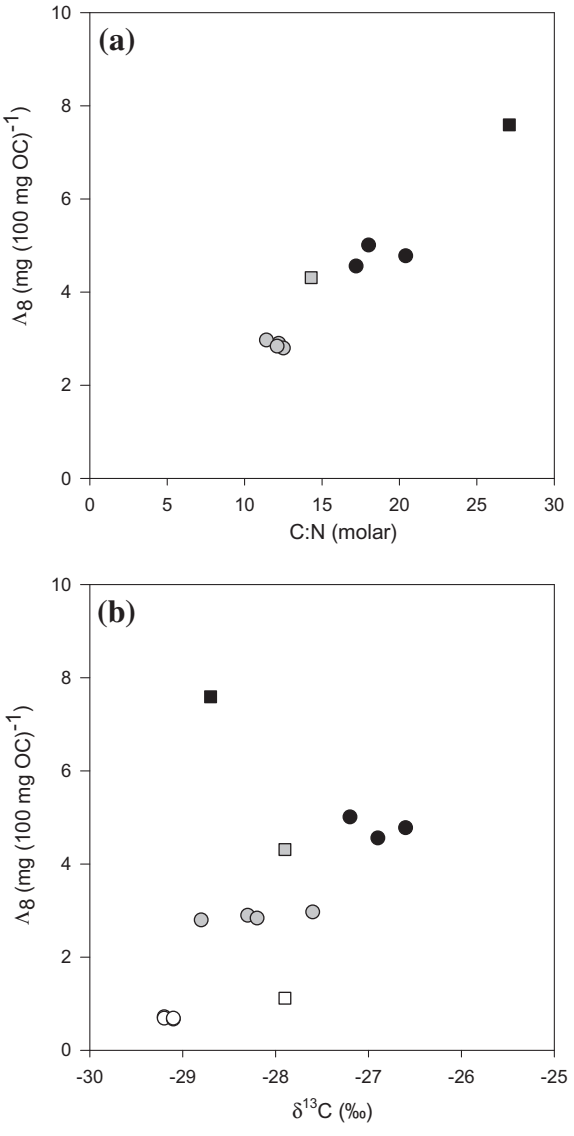

Fig. 4. (a) Carbon-normalized lignin yields (Λ_8) versus C:N (molar) and; (b) δ^{13}C. CPOM = black symbols; sites 1,2 and 4 (circles) and site 5 (square). FPOM = gray symbols; sites 1–4 (circles) and site 5 (square). DOM = white symbols; sites 1–4 (circles) and site 5 (square).

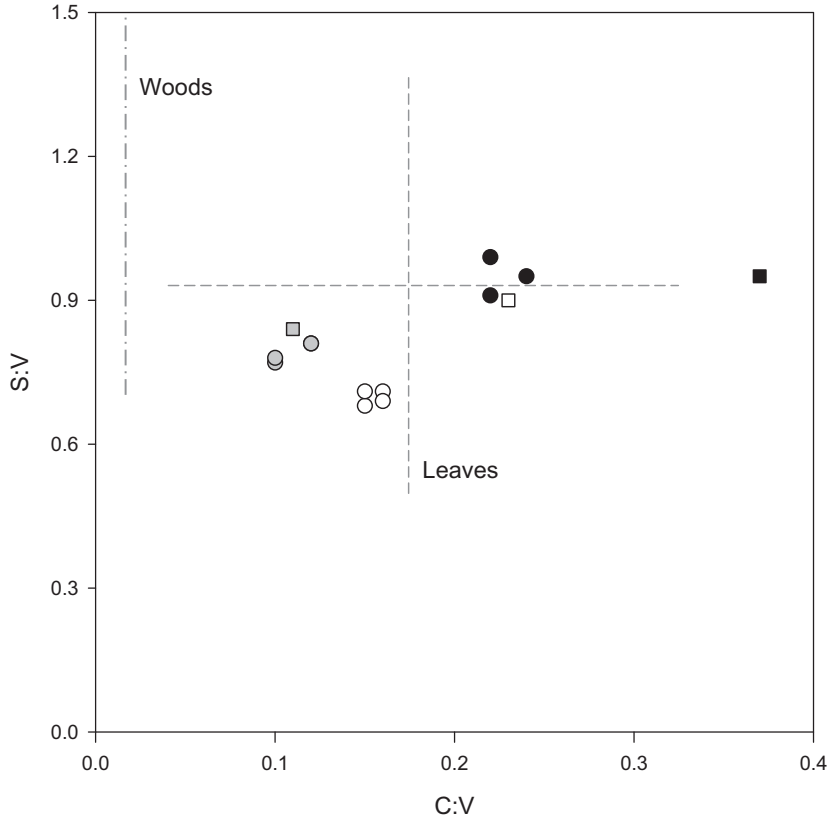

Fig. 5. Lignin compositional parameters, S:V versus C:V. CPOM = black symbols; sites 1,2 and 4 (circles), site 5 (square). FPOM = gray symbols; sites 1–4 (circles), site 5 (square). DOM = white symbols; sites 1–4 (circles) and site 5 (square). Gray dashed cross and gray dash-dot line represent the median and range of values measured for dicotyledonous plant leaves and woody tissues by Hedges et al. (1986) respectively.

(S:V) and nonwoody and woody tissues (C:V) (Fig. 5; Hedges and Mann, 1979). Congo CPOM and FPOM S:V and FPOM C:V ratios are comparable to those found in the Amazon Rivers, whereas CPOM C:V ratios appear to be slightly higher in the Congo (Hedges et al., 1986,2000). Thus higher C:V values in the Congo could be due to the presence of more grass tissue in the CPOM as site 5 (savannah tributary), shows the highest C:V (0.37) of all sites and grasses are known to have a high C:V near 1.0 (Hedges et al., 1986), although $\delta^{13}C$ does not show any C_4 shift (Table 3). The Congo CPOM S:V and C:V ratios were higher than the FPOM values which could be explained by more woody material and grass tissue in the CPOM relative to the FPOM respectively. Aufdenkampe et al. (2007) also noted decreasing C:V from CPOM to FPOM at a range of sites in the Amazon and suggested this could be a function of selective degradation or partitioning. Overall though for all OM fractions the dominant sources appear to be leaf material (angiosperm nonwoody sources) and some woody material (Fig. 5; Hedges and Mann, 1979; Hedges et al., 1986).

The $(Ad:Al)_v$ and $(Ad:Al)_s$ ratios of OM have been used to examine degradation state, with higher ratios indicative of increased degradation in time series (Opsahl and Benner, 1995; Hernes and Benner, 2003; Spencer et al., 2009). Congo CPOM and FPOM have higher ratios than the same fractions in Amazon Basin Rivers, potentially reflecting a greater degree of degradation within the particulate fractions (Table 4; Hedges et al., 1986). For example, Amazon mainstem CPOM and FPOM $(Ad:Al)_v$ values were 0.23 and 0.44 (Hedges et al., 1986), versus 0.52 and 1.14 respectively for the Congo mainstem sites (Table 4). The elevated $(Ad:Al)_v$ and $(Ad:Al)_s$ values for Congo DOM are likely a function of fractionation effects on the dissolved phase due to leaching and sorption as described above and thus do not necessarily reflect a greater degree of degradation (Hernes et al., 2007). In riverine sediment studies the $(Ad:Al)_v$ has particularly received attention due to their higher relative yields and thus more accurate quantification in comparison to syringyl phenols. To further investigate POM dynamics in the Congo $(Ad:Al)_v$ was examined against C:N and $\Delta^{14}C$ (Fig. 6). The high lignin $(Ad:Al)_v$ values associated with nitrogen enrichment and $\Delta^{14}C$ depletion in the FPOM present a strong argument for the source of FPOM as soil derived mineral associated OM, whereas the CPOM appears to be primarily derived from recent vegetation inputs dominated by a C_3 signal (Hedges et al., 1986; Hedges and Oades, 1997).

4.4. Congo River organic matter biogeochemistry

The Congo is clearly an organic rich river, dominated by DOM and although its TSS concentration is low it is carbon rich. In terms of both DOM and POM the Congo

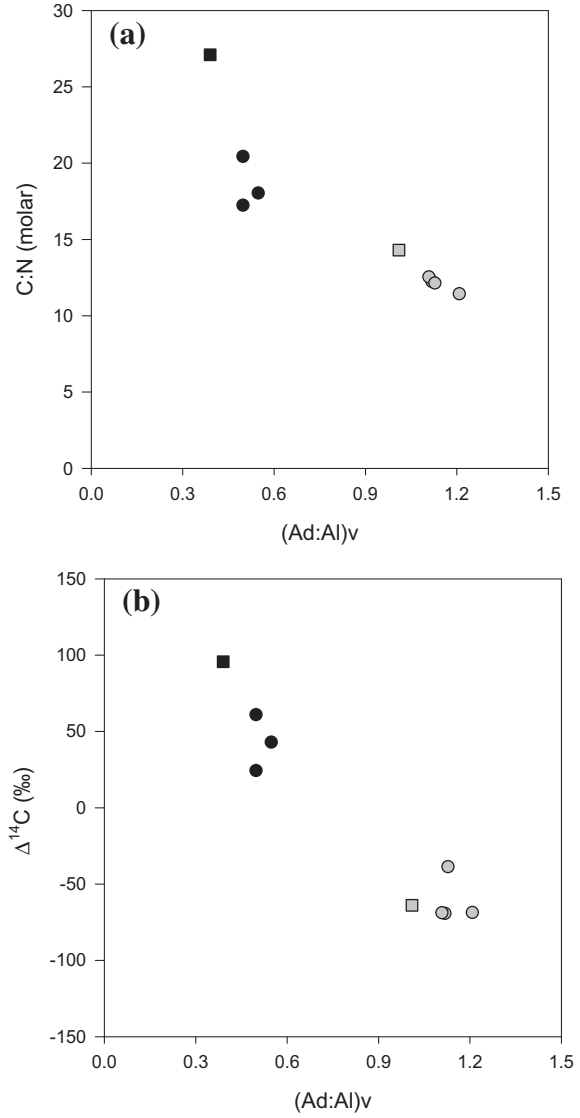

Fig. 6. (a) Lignin diagenetic parameter, $(Ad:Al)_v$ versus C:N (molar) and; (b) $\Delta^{14}C$. CPOM = black symbols; sites 1,2 and 4 (circles) and site 5 (square). FPOM = gray symbols; sites 1–4 (circles) and site 5 (square).

appears to be a major exporter of terrigenous derived OM as evidenced by high Λ_8 values and in this respect is similar to other major tropical rivers (Hedges et al., 1986,2000; Alin et al., 2008). Congo CPOM and FPOM appear to have different sources with the FPOM fraction principally soil derived mineral associated OM as evidenced by its nitrogen enrichment, high lignin $(Ad:Al)_v$ ratios and depleted $\Delta^{14}C$ signature; in contrast, CPOM originates from modern vegetation inputs dominated by a C_3 signal (Figs. 4 and 6; Hedges et al., 1986; Hedges and Oades, 1997). FPOM in the Congo appears to be heavily degraded as further evidenced by its low Λ_8 in relation to CPOM, elevated (Ad:Al) ratios and the high relative degree of enrichment in its $\delta^{15}N$ isotopic values (Tables 3 and 4). Although there is not a great difference in radiocarbon age between the small savannah tributary (site 5) and the mainstem sites (1–4) there is some evidence for in-river biogeochemical or physical processing (e.g. sorption) as CPOM and FPOM from site 5 have lower $\delta^{15}N$ values, higher C:N values, lower (Ad:Al) ratios and greater Λ_8 in relation to any mainstem sites (Tables 3 and 4). However, as we are only comparing one site from one season to the mainstem sites, we recognize that future studies are required to assess both greater spatial and temporal variability with respect to comprehensively addressing OM processing in the Congo River Basin. The FPOM fraction may potentially undergo extended degradation in the Cuvette Congolaise, which has been shown to act as a giant sediment trap and consequently impacts biogeochemical processes (Laraque et al., 2009), and to a lesser extent within the Malebo Pool.

Little evidence of OM degradation or variation between samples was observed in mainstem sites 1–4, with the implication that future studies aimed at examining Congo River export to the Atlantic Ocean can focus on site 2. This is logistically much more feasible as it is adjacent to the major urban centers of Kinshasa (D.R. Congo) and Brazzaville (Republic of Congo). In particular, proximity to major infrastructure will better allow for the kind of time series sampling that will be critical for understanding seasonal processing and dynamics of OM within the Congo River Basin as well as investigating the impacts of ongoing local and global change. The clear indication that FPOM is derived from soils points toward the need to identify and investigate the primary contributing soils. Future work is also required to better define the fate of Congo derived OM in the Atlantic Ocean at this major site for OM burial (Rabouille et al., 2009). Finally, as OM exported by the Congo is predominantly modern (Table 4), which has been shown to be the dominant source of excess CO_2 in the Amazon (Mayorga et al., 2005), and as the Congo has a vast seasonally inundated flooded area the need for future studies to quantify this carbon flux especially while the Congo as yet remains the most pristine major tropical rainforest basin are acute.

ACKNOWLEDGMENTS

We thank the Regie de Voies Fluviales in Kinshasa (D.R. Congo) for providing hydrology data and Kevin Burkhill at the University of Birmingham for producing Fig. 1. This study was supported by a NERC radiocarbon grant (#1244.1007) to RGMS and AB and discretionary funds awarded to JS by the Department of Plant Sciences, UC Davis. RGMS and JS are very grateful to Richard N. Tshibambe for facilitating the required visas and permits and Lodi Jean Paul Lama for their assistance in the D.R. Congo. Finally, we wish to sincerely thank three anonymous reviewers and the Associate Editor Prof. J. Middelburg who provided helpful comments that improved this manuscript.

REFERENCES

Ahad J. M. E., Ganeshram R. S., Spencer R. G. M., Uher G., Gulliver P. and Bryant C. L. (2006) Evidence for anthropogenic ^{14}C-enrichment in estuarine waters adjacent to the North Sea. *Geophys. Res. Lett.* **33**, L08608. doi:10.1029/2006GL025991.

Aitkenhead J. A. and McDowell W. H. (2000) Soil C:N ratio as a predictor of annual riverine DOC flux at local and global scales. *Global Biogeochem. Cycles* **14**, 127–138.

Alin S. R., Aalto R., Goni M. A., Richey J. R. and Dietrich W. E. (2008) Biogeochemical characterization of carbon sources in the Strickland and Fly rivers, Papua New Guinea. *J. Geophys. Res. Earth Surf.* **113**, F01S05. doi:10.1029/2006JF000625.

Aragao L. E. O. C. and Shimabukuro Y. E. (2010) The incidence of fire in Amazonian forest with implications for REDD. *Science* **328**, 1275–1278.

Aufdenkampe A. K., Hedges J. I., Richey J. E., Krusche A. V. and Llerena C. A. (2001) Sorptive fractionation of dissolved organic nitrogen and amino acids onto fine sediments within the Amazon Basin. *Limnol. Oceanogr.* **46**, 1921–1935.

Aufdenkampe A. K., Mayorga E., Hedges J. I., Llerena C., Quay P. D., Gudeman J., Krusche A. V. and Richey J. E. (2007) Organic matter in the Peruvian headwaters of the Amazon: compositional evolution from the Andes to the lowland Amazon mainstem. *Org. Geochem.* **38**, 337–364.

Aufdenkampe A. K., Mayorga E., Raymond P. A., Melack J. M., Doney S. C., Alin S. R., Aalto R. E. and Yoo K. (2011) Riverine coupling of biogeochemical cycles between land, oceans, and atmosphere. *Front. Ecol. Environ.* **9**, 53–60.

Baccini A., Laporte N., Goetz S. J., Sun M. and Dong H. (2008) A first map of tropical Africa's above-ground biomass derived from satellite imagery. *Environ. Res. Lett.* **3**, 045011.

Battin T. J., Kaplan L. A., Findlay S., Hopkinson C. S., Marti E., Packman A. I., Newbold J. D. and Sabater F. (2008) Biophysical controls on organic carbon fluxes in fluvial networks. *Nat. Geosci.* **1**, 95–100.

Battin T. J., Luyssaert S., Kaplan L. A., Aufdenkampe A. K., Richter A. and Tranvik L. J. (2009) The boundless carbon cycle. *Nat. Geosci.* **2**, 598–600.

Benner R., Benitez-Nelson B., Kaiser K. and Amon R. M. W. (2004) Export of young terrigenous dissolved organic carbon from rivers to the Arctic Ocean. *Geophys. Res. Lett.* **31**, L05305. doi:10.1029/2003GL019251.

Bouillon S., Abril G., Borges A. V., Dehairs F., Govers G., Hughes H. J., Merckx R., Meysman F. J. R., Nyunja J., Osburn C. and Middelburg J. J. (2009) Distribution, origin and cycling of carbon in the Tana River (Kenya): a dry season basin-scale survey from headwaters to the delta. *Biogeosciences* **6**, 2475–2493.

Boutton T. W., Wong W. W., Hachey D. L., Lee L. S., Cabrera M. P. and Klein P. D. (1983) Comparison of quartz and pyrex tubes for combustion of organic samples for stable carbon isotope analysis. *Anal. Chem.* **55**, 1832–1833.

Cadee G. C. (1984) Particulate and dissolved organic carbon and chlorophyll-a in the Zaire River, estuary and plume. *Neth. J. Sea Res.* **17**, 426–440.

Coe M. T., Costa M. H. and Soares-Filho B. S. (2009) The influence of historical and potential future deforestation on the stream flow of the Amazon River – Land surface processes and atmospheric feedbacks. *J. Hydrol.* **369**, 165–174.

Coe M. T., Latrubesse E. M., Ferreira M. E. and Amsler M. L. (2011) The effects of deforestation and climate variability on the streamflow of the Araguaia River, Brazil. *Biogeochemistry*. doi:10.1007/s10533-011-9582-2.

Cole J. J., Prairie Y. T., Caraco N. F., McDowell W. H., Tranvik L. J., Striegl R. G., Duarte C. M., Kortelainen P., Downing J. A., Middelburg J. J. and Melack J. (2007) Plumbing the global carbon cycle: integrating inland waters into the terrestrial carbon budget. *Ecosystems* **10**, 171–184.

Coplen T. B., Brand W. A., Gehre M., Groning M., Meijer H. A., Toman B. and Verkouteren R. M. (2006) New guidelines for delta ^{13}C measurements. *Anal. Chem.* **78**, 2439–2441.

Coynel A., Seyler P., Etcheber H., Meybeck M. and Orange D. (2005) Spatial and seasonal dynamics of total suspended sediment and organic carbon species in the Congo River. *Global Biogeochem. Cycles* **19**, GB4019. doi:10.1029/2004GB002335.

Eisma D. and Van Bennekom A. J. (1978) The Zaire River and estuary and the Zaire outflow in the Atlantic Ocean. *Neth. J. Sea Res.* **12**, 255–272.

Galy V., France-Lanord C., Beyssac O., Faure P., Kudrass H. and Palhol F. (2007) Efficient organic carbon burial in the Bengal fan sustained by the Himalayan erosional system. *Nature* **450**, 407–410.

Galy V., France-Lanord C. and Lartiges B. (2008) Loading and fate of particulate organic carbon from the Himalaya to the Ganga–Brahmaputra delta. *Geochim. Cosmochim. Acta* **72**, 1767–1787.

Hedges J. I. and Ertel J. R. (1982) Characterization of lignin by gas capillary chromatography of cupric oxide oxidation-products. *Anal. Chem.* **54**, 174–178.

Hedges J. I. and Mann D. C. (1979) Characterization of plant tissues by their lignin oxidation products. *Geochim. Cosmochim. Acta* **43**, 1803–1807.

Hedges J. I. and Oades J. M. (1997) Comparative organic geochemistries of soils and marine sediments. *Org. Geochem.* **27**, 319–361.

Hedges J. I., Clark W. A., Quay P. D., Richey J. E., Devol A. H. and Santos U. D. M. (1986) Compositions and fluxes of particulate organic material in the Amazon River. *Limnol. Oceanogr.* **31**, 717–738.

Hedges J. I., Cowie G. L., Richey J. E., Quay P. D., Benner R., Strom M. and Forsberg B. R. (1994) Origins and processing of organic matter in the Amazon River as indicated by carbohydrates and amino acids. *Limnol. Oceanogr.* **39**, 743–761.

Hedges J. I., Keil R. G. and Benner R. (1997) What happens to terrestrial organic matter in the ocean? *Org. Geochem.* **27**, 195–212.

Hedges J. I., Mayorga E., Tsamakis E., McClain M. E., Aufdenkampe A. K., Quay P., Richey J. E., Benner R., Opsahl S., Black B., Pimental T., Quintanilla J. and Maurice L. (2000) Organic matter in Bolivian tributaries of the Amazon River: a comparison to the lower main stream. *Limnol. Oceanogr.* **45**, 1449–1466.

Hernes P. J. and Benner R. (2003) Photochemical and microbial degradation of dissolved lignin phenols: implications for the fate of terrigenous dissolved organic matter in marine environments. *J. Geophys. Res. [Oceans]* **108**, 3291. doi:10.1029/2002JC001421.

Hernes P. J., Robinson A. C. and Aufdenkampe A. K. (2007) Fractionation of lignin during leaching and sorption and implications for organic matter "freshness". *Geophys. Res. Lett.* **34**, L17401. doi:10.1029/2007GL031017.

Holmes R. M., McClelland J. W., Raymond P. A., Frazer B. B., Peterson B. J. and Stieglitz M. (2008) Lability of DOC transported by Alaskan rivers to the Arctic Ocean. *Geophys. Res. Lett.* **35**, L03402. doi:10.1029/2007GL032837.

Kasier K. and Guggenberger G. (2003) Mineral surfaces and soil organic matter. *Eur. J. Soil Sci.* **54**, 219–236.

Koenig R. (2008) Critical time for African rainforests. *Science* **320**, 1439–1441.

Laporte N., Stabach J. A., Grosch R., Lin T. S. and Goetz S. J. (2007) Expansion of industrial logging in Central Africa. *Science* **316**, 1451.

Laraque A., Bricquet J. P., Pandi A. and Olivry J. C. (2009) A review of material transport by the Congo River and its tributaries. *Hydrol. Processes* **23**, 3216–3224.

Ludwig W. and Probst J. L. (1998) River sediment discharge to the oceans: present-day controls and global budgets. *Am. J. Sci.* **298**, 265–295.

Mariotti A., Francois G., Giresse P. and Mouzeo K. (1991) Carbon isotope composition and geochemistry of particulate organic

matter in the Congo River (Central Africa): application to the study of Quaternary sediments off the mouth of the river. *Chem. Geol.* **86**, 345–357.

Mayorga E., Aufdenkampe A. K., Masiello C. A., Krusche A. V., Hedges J. I., Quay P. D., Richey J. E. and Brown T. A. (2005) Young organic matter as a source of carbon dioxide outgassing from Amazonian rivers. *Nature* **436**, 538–541.

McGroddy M. E., Daufresne T. and Hedin L. O. (2004) Scaling of C:N:P stoichiometry in forests worldwide: implications of terrestrial redfield-type ratios. *Ecology* **85**, 2390–2401.

Nadelhoffer K. J. and Fry B. (1988) Controls on natural nitrogen-15 and carbon-13 abundances in forest soil organic matter. *Soil Sci. Soc. Am. J.* **52**, 1633–1640.

Opsahl S. and Benner R. (1995) Early diagenesis of vascular plant tissues, lignin and cutin decomposition and biogeochemical implications. *Geochim. Cosmochim. Acta* **59**, 4889–4904.

Osburn C. L. and St-Jean G. (2007) The use of wet chemical oxidation with high-amplification isotope ratio mass spectrometry (WCO-IRMS) to measure stable isotope values of dissolved organic carbon in seawater. *Limnol. Oceanogr.* **5**, 296–308.

Pak H., Zaneveld J. R. V. and Spinrad R. W. (1984) Vertical distribution of suspended particulate matter in the Zaire River, estuary and plume. *Neth. J. Sea Res.* **17**, 412–425.

Post W. M., Pastor J., Zinke P. J. and Stangenberger A. G. (1985) Global patterns of soil nitrogen storage. *Nature* **317**, 613–616.

Prunier, G. (2008) Africa's World War: Congo, the Rwandan genocide, and the making of a continental catastrophe. Oxford University Press, pp. 576.

Qualls R. and Haines B. L. (1992) Measuring adsorption isotherms using continuous, unsaturated flow through intact soil cores. *Soil Sci. Soc. Am. J.* **56**, 456–460.

Rabouille C., Caprais J. C., Lansard B., Crassous P., Dedieu K., Reyss J. L. and Khripounoff A. (2009) Organic matter budget in the Southeast Atlantic continental margin close to the Congo Canyon: in situ measurements of sediment oxygen consumption. *Deep Sea Res. Part II* **56**, 2223–2238.

Raymond P. A. and Bauer J. E. (2001) Riverine export of aged terrestrial organic matter to the North Atlantic Ocean. *Nature* **409**, 497–500.

Raymond P. A., McClelland J. W., Holmes R. M., Zhulidov A. V., Mull K., Peterson B. J., Striegl R. G., Aiken G. R. and Gurtovaya T. Y. (2007) Flux and age of dissolved organic carbon exported to the Arctic Ocean: a carbon isotopic study of the five largest rivers. *Global Biogeochem. Cycles* **21**, GB4011. doi:10.1029/2007GB002934.

Richey J. E., Meade R. H., Salati E., Devol A. H., Nordin C. F. and Santos U. D. (1986) Water discharge and suspended sediment concentrations in the Amazon River: 1982–1984. *Water Resour. Res.* **22**, 756–764.

Richey J. E., Melack J. M., Aufdenkampe A. K., Ballester V. M. and Hess L. L. (2002) Outgassing from Amazonian rivers and wetlands as a large tropical source of atmospheric CO_2. *Nature* **416**, 617–620.

Runge J. (2007) The Congo River, Central Africa. In *Large Rivers: Geomorphology and Management* (ed. A. Gupta), pp. 293–309. Large Rivers: Geomorphology and Management. Wiley.

Soares-Filho B. S., Nepstad D. C., Curran L. M., Cerqueira G. C., Garcia R. A., Ramos C. A., Voll E., McDonald A., Lefebvre P. and Schlesinger P. (2006) Modelling conservation in the Amazon basin. *Nature* **440**, 520–523.

Spencer R. G. M., Aiken G. R., Wickland K. P., Striegl R. G. and Hernes P. J. (2008) Seasonal and spatial variability in dissolved organic matter quantity and composition from the Yukon River basin, Alaska. *Global Biogeochem. Cycles* **22**, GB4002. doi:10.1029/2008GB003231.

Spencer R. G. M., Stubbins A., Hernes P. J., Baker A., Mopper K., Aufdenkampe A. K., Dyda R. Y., Mwamba V. L., Mangangu J. N., Wabakanghanzi J. N. and Six J. (2009) Photochemical degradation of dissolved organic matter and dissolved lignin phenols from the Congo River. *J. Geophys. Res. Biogeosci.* **114**, G03010. doi:10.1029/2009JG000968.

Spencer R. G. M., Hernes P. J., Ruf R., Baker A., Dyda R. Y., Stubbins A. and Six J. (2010a) Temporal controls on dissolved organic matter and lignin biogeochemistry in a pristine tropical river, Democratic Republic of Congo. *J. Geophys. Res. Biogeosci.* **115**, G03013. doi:10.1029/2009JG001180.

Spencer R. G. M., Aiken G. R., Dyda R. Y., Butler K. D., Bergamaschi B. A. and Hernes P. J. (2010b) Comparison of XAD with other dissolved lignin isolation techniques and a compilation of analytical improvements for the analysis of lignin in aquatic settings. *Org. Geochem.* **41**, 445–453.

Striegl R. G., Dornblaser M. M., Aiken G. R., Wickland K. P. and Raymond P. A. (2007) Carbon export and cycling by the Yukon, Tanana, and Porcupine rivers, Alaska, 2001–2005. *Water Resour. Res.* **43**, W02411. doi:10.1029/2006WR005201.

Stubbins A., Spencer R. G. M., Chen H., Hatcher P. G., Mopper K., Hernes P. J., Mwamba V. L., Mangangu A. M., Wabakanghanzi J. N. and Six J. (2010) Illuminated darkness: molecular signatures of Congo River dissolved organic matter and its photochemical alteration as revealed by ultrahigh precision mass spectrometry. *Limnol. Oceanogr.* **55**, 1467–1477.

Stuiver M. and Polach H. A. (1977) Reporting of ^{14}C data. *Radiocarbon* **19**, 355–363.

Sys C. (1960) *Carte des Sols du Congo Belge et du Ruanda-Urundi (1:5M)*. Institut National pour l'Etude Agronomique du Congo Belge, Brussels.

Trumbore S. (2000) Age of soil organic matter and soil respiration: radiocarbon constraints on belowground C dynamics. *Ecol. Appl.* **10**, 399–411.

van der Plicht J. and Hogg A. (2006) A note on reporting radiocarbon. *Quat. Geochronol.* **1**, 237–240.

Associate editor: Jack J. Middelburg